Crystallization Kinetics and Melting Behavior of Nylon 10,10 in Nylon 10,10–Montmorillonite Nanocomposites

Guosheng Zhang, Deyue Yan

College of Chemistry and Chemical Engineering, Shanghai Jiao Tong University, 800 Dongchuan Road, Shanghai 200240, People's Republic of China

Received 2 May 2002; accepted 27 June 2002

ABSTRACT: The crystallization kinetics and melting behavior of nylon 10,10 in neat nylon 10,10 and in nylon 10,10–montmorillonite (MMT) nanocomposites were systematically investigated by differential scanning calorimetry. The crystallization kinetics results show that the addition of MMT facilitated the crystallization of nylon 10,10 as a heterophase nucleating agent; however, when the content of MMT was high, the physical hindrance of MMT layers to the motion of nylon 10,10 chains retarded the crystallization of nylon 10,10, which was also confirmed by polarized optical microscopy. However, both nylon 10,10 and nylon 10,10–MMT nanocomposites exhibited multiple melting behavior under isothermal and nonisothermal crystallization conditions. The temperature of the lower melting peak (peak I) was independent of MMT content and almost remained constant; however, the temperature of the highest melting peak (peak II) decreased with increasing MMT content due to the physical hindrance of MMT layers to the motion of nylon 10,10 chains. © 2003 Wiley Periodicals, Inc. J Appl Polym Sci 88: 2181–2188, 2003

Key words: crystallization; kinetics (polym.); nylon; nanocomposites; differential scanning calorimetry (DSC)

INTRODUCTION

Nylon–montmorillonite (MMT) nanocomposites[1–5] have attracted much attention because of their outstanding properties, including a high modulus,[2–5] a high heat distortion temperature,[2–4] good barrier properties of water,[6] and fireproof properties.[7] Nylon 10,10 is one of the important polyamide engineering plastics that has been produced commercially in China since the 1970s. It has a high strength, elasticity, toughness, and abrasion resistance;[8] however, it also has some of the inherent drawbacks of nylons due to its polar amide bonds, such as a lower modulus and a higher moisture absorption. However, it is possible to overcome these drawbacks through the preparation of a nylon 10,10–MMT nanocomposite. Recently, nylon 10,10–MMT nanocomposites have been prepared successfully by intercalating polymerization in our lab, and this nanocomposite has a higher modulus and onset temperature of decomposition compared with neat nylon 10,10.[9]

It is well known that nylon is a semicrystalline polymer. The crystallization kinetics and melting behavior of nylon 10,10 in nylon 10,10–MMT nanocomposites are worth studying as a new material with a potential value of application, even though there are many reports on the crystallization kinetics[10–14] and melting behavior[15–25] of neat nylons. In this study, the crystallization kinetics and melting behavior of nylon 10,10 in nylon 10,10–MMT nanocomposites were investigated by differential scanning calorimetry (DSC).

Correspondence to: D. Yan (dyyan@mail.sjtu.edu.cn).

Journal of Applied Polymer Science, Vol. 88, 2181–2188 (2003)

EXPERIMENTAL

Materials and preparation

The nylon 10,10–MMT nanocomposite was prepared by intercalating polymerization.[9] The MMT was firstly modified with 11-aminoundecanoic acid. Then, it was mixed with 10,10 salt. The nanocomposites were synthesized by typical melting polycondensation. The MMT contents were 1 wt % (1010-1), 6 wt % (1010-6), and 10 wt % (1010-10). The neat nylon 10,10 (1010-0) was synthesized by the same polymerization procedure for the purpose of comparison. A sample with a thickness of 0.2 mm was obtained by hot molding at 220°C for several minutes followed by quenching to room temperature.

DSC measurement

All measurements were performed using a PerkinElmer Pyris-1 differential scanning calorimeter (USA) under a nitrogen purge, and the temperature was calibrated with indium. Sample weight varied from 5 to 6 mg.

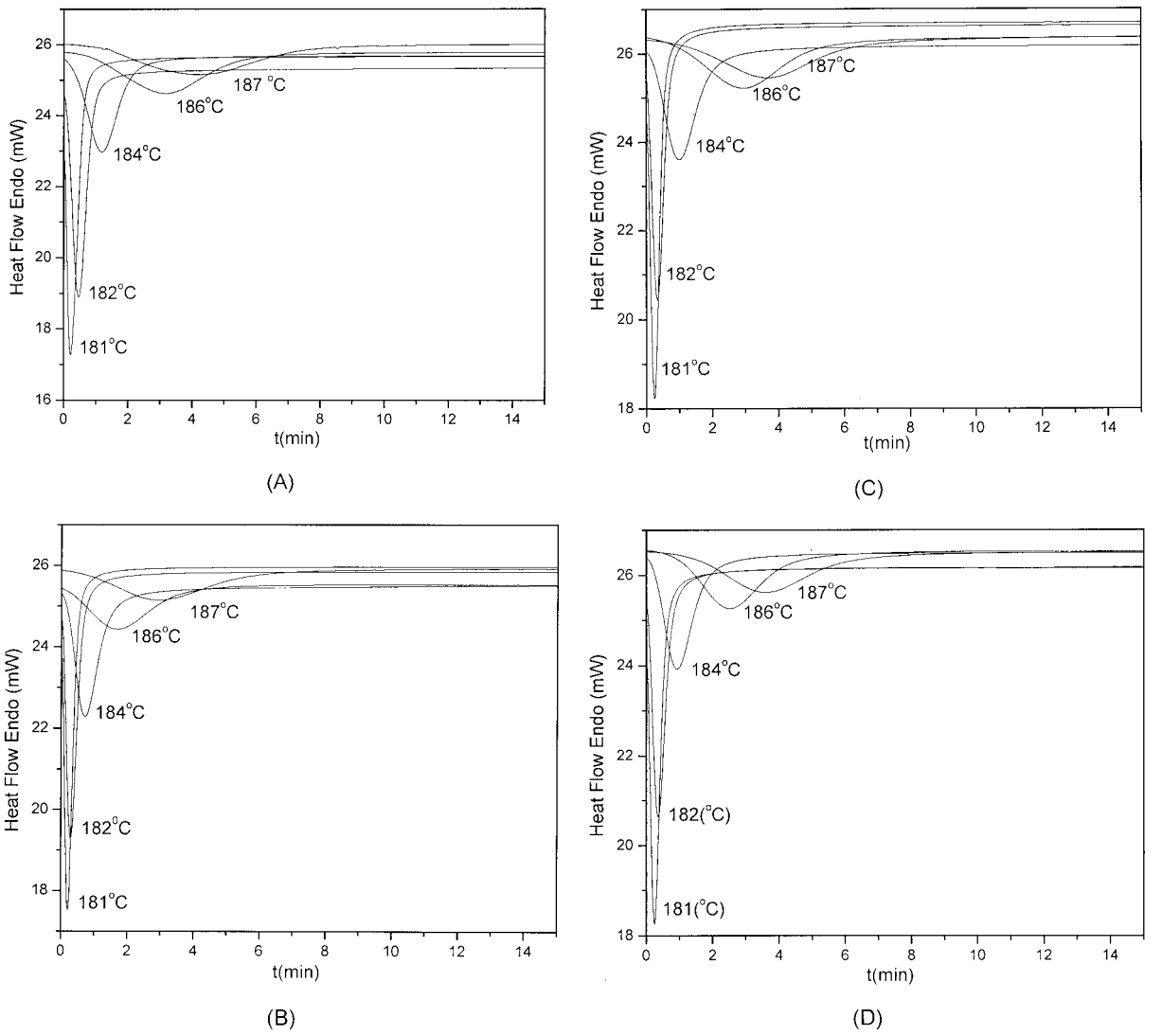

Figure 1 Heat flow versus time during the isothermal crystallization of (A) 1010-0, (B) 1010-1, (C) 1010-6, and (D) 1010-10 at specified T_c's by DSC.

Isothermal crystallization from the melt was carried out by heating the sample (20°C/min) to 230°C for 10 min to eliminate residual crystals, then cooling it quickly (−100°C/min) to the predetermined crystallization temperature (T_c), and isothermally crystallizing it for 30 min in a temperature range of 181 to 187°C. The exothermic curves of heat flow as a function of time were recorded. Finally, the sample was heated to 230°C at 10°C/min to investigate the melting behavior under the isothermal crystalline process.

In the case of nonisothermal crystallization, the sample was heated to 230°C at 20°C/min and held there for 10 min, then cooled to 50°C at a rate of 10°C/min, and finally heated to 230°C again at 10°C/min. The cooling and the second heating scanning processes were recorded to investigate the nonisothermal crystallization and melting behavior, respectively.

Polarized optical microscope observations

Morphological observations were performed on a Leica polarized optical microscope (Germany) equipped with a temperature-controlled stage.

RESULTS AND DISCUSSION

Isothermal crystallization kinetics analysis

Figure 1 shows the isothermal crystallization DSC curves for neat nylon 10,10 and nylon 10,10–MMT nanocomposites. All the sample were heated to 230°C at the rate of 20°C/min, held there for 10 min to destroy all residual crystals, and then cooled (100°C/min) to various T_c's. With the increase of T_c, the crystallization exothermic peak shifted to longer times and became flatter in both neat nylon 10,10 and nylon

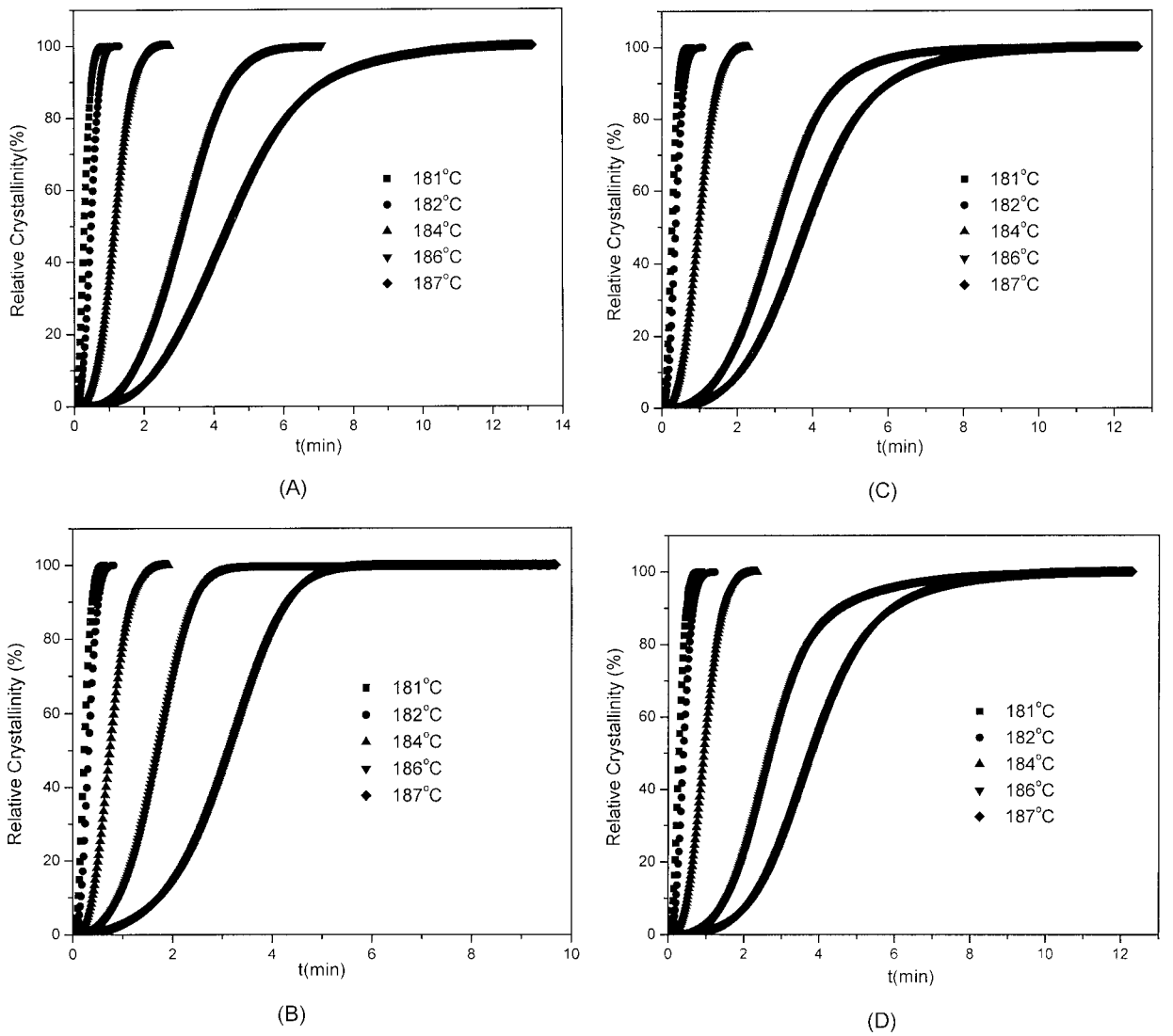

Figure 2 *Xt* at different times in the process of isothermal crystallization on (A) 1010-0, (B) 1010-1, (C) 1010-6, and (D) 1010-10.

10,10–MMT nanocomposites, which indicates that the total crystallization time was lengthened and that the crystallization rate decreased with increasing T_c.

Figure 2 shows the relative crystallinity (Xt) for different crystallization times. The Avrami equation[26,27] can be used to analyze the isothermal crystallization process of semicrystalline polymers as shown:

$$Xt = 1 - \exp(-Kt^n)$$

or

$$\log[-\ln(1 - Xt)] = n \log t + \log K \qquad (1)$$

where t is crystallization time, K is the crystallization rate parameter and n is the Avrami parameter.

The double logarithmic plot of $\log[-\ln(1 - Xt)]$ versus $\log t$ is shown in Figure 3. A pretty good linear relation for the isothermal crystallization was observed, and there was no rolloff at longer times, which implies that the secondary crystallization of nylon 10,10 did not occur in both neat nylon 10,10 and the nanocomposites under the experimental conditions.

The values of n and K can be determined by fitting the linear line of $\log[-\ln(1 - Xt)]$ versus $\log t$, and they are listed in Table I. n varied from 2.4 to 2.9 in both neat nylon 10,10 and the nanocomposites, depending on T_c. However, the value K increased with decreasing T_c of the same sample, which indicates that the addition of MMT apparently did not change the crystallization mechanism of nylon 10,10.

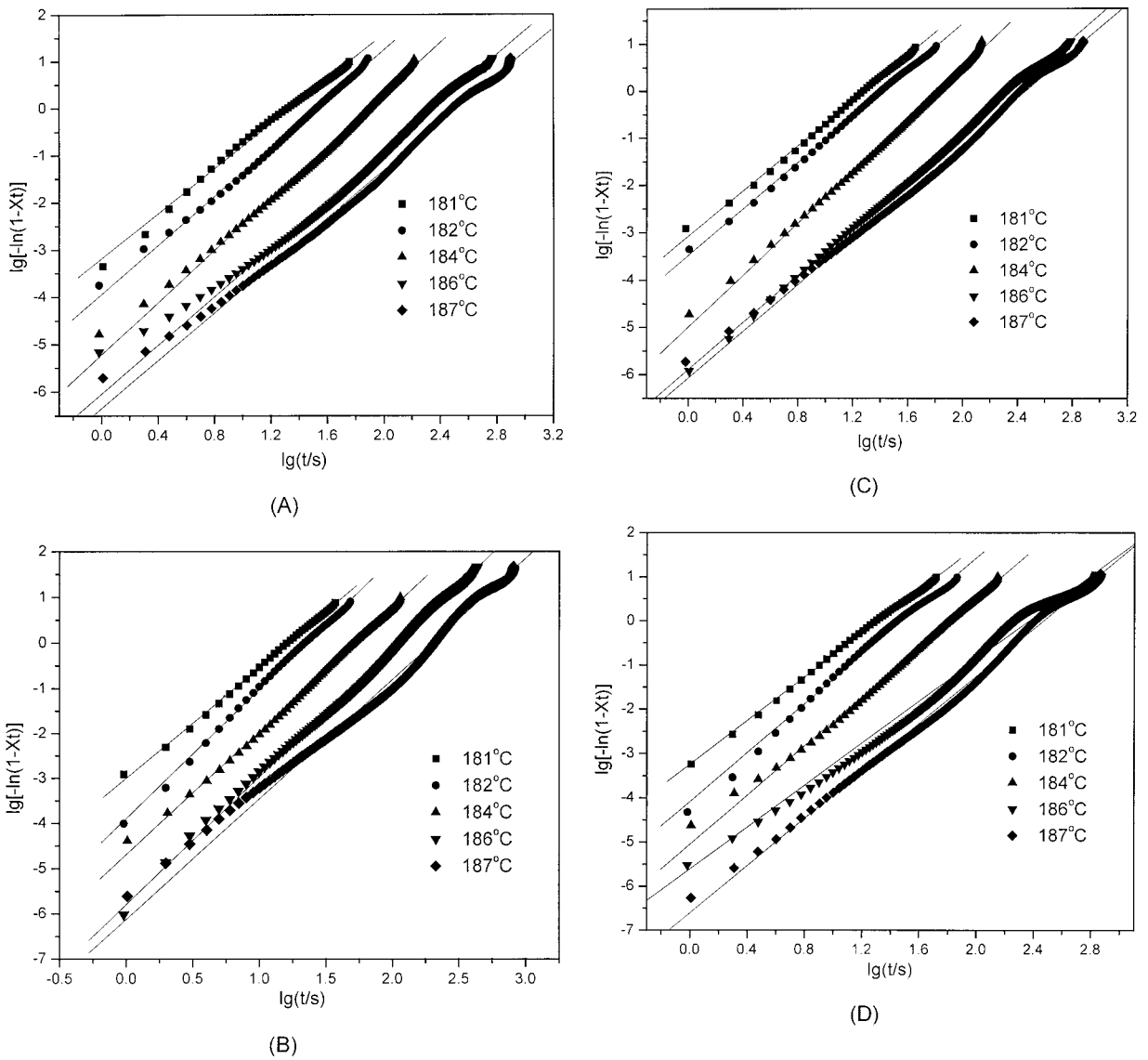

Figure 3 Plots of log[−ln(1 − *Xt*)] versus log *t* for the isothermal crystallization of (A) 1010-0, (B) 1010-1, (C) 1010-6, and (D) 1010-10 at different temperatures.

The *crystallization half-time* ($t_{1/2}$) is defined as the time at which the crystallinity reaches 50%. It can be determined from the measured kinetics parameters:

$$t_{1/2} = (\ln 2/K)^{1/n} \quad (2)$$

Usually the rate of crystallization (G) can be defined as the reciprocal of $t_{1/2}$, that is, $G = \tau_{1/2} = 1/t_{1/2}$; the values of both $t_{1/2}$ and $\tau_{1/2}$ are listed in Table I.

It is shown in Table I that the crystallization rate of nylon 10,10 in the nanocomposites, $\tau_{1/2}$, was faster than for the neat nylon 10,10, which could be ascribed to the effects of MMT as an efficient nucleating agent to facilitate nylon 10,10 crystallization. It is interesting that the crystallization rate of nylon 10,10 in 1010-6 and 1010-10 was slower than that in 1010-1 and similar to that in neat nylon 10,10, which implies that the presence of MMT also tended to retard the nylon 10,10 crystallization. It is evident that the MMT played two roles in the crystallization of nylon 10,10: a heterophase nucleating agent to facilitate the crystallization and a physical hindrance to retard the crystallization. When the content of MMT was high, only a part of MMT played the role of the nucleating agent, and the physical hindrance became more serious. So the crystallization rates of 1010-6 and 1010-10 began to slow down but were still faster than that of neat nylon 10,10.

Nonisothermal crystallization kinetics analysis

The practical processes are usually performed under nonisothermal conditions, so it is of practical signifi-

TABLE I
Parameters of Isothermal Crystallization

Sample	T_c (°C)	n	$-\log K$	$t_{1/2}$ (min)	$\tau_{1/2}$ (min^{-1})
1010-0	181	2.4	3.18	0.31	3.23
1010-0	182	2.6	3.94	0.48	2.08
1010-0	184	2.8	5.22	1.14	0.88
1010-0	186	2.6	6.04	3.25	0.31
1010-0	187	2.5	6.35	4.78	0.21
1010-1	181	2.5	3.00	0.24	4.17
1010-1	182	2.9	3.89	0.33	3.03
1010-1	184	2.7	4.69	0.76	1.32
1010-1	186	2.8	5.79	1.65	0.61
1010-1	187	2.7	6.12	2.91	0.34
1010-6	181	2.4	2.40	0.27	3.70
1010-6	182	2.5	2.46	0.37	2.70
1010-6	184	2.7	2.75	0.96	1.04
1010-6	186	2.5	2.50	3.25	0.31
1010-6	187	2.5	2.47	4.11	0.24
1010-10	181	2.5	2.47	0.30	3.33
1010-10	182	2.8	2.76	0.44	2.27
1010-10	184	2.8	2.78	0.96	1.04
1010-10	186	2.4	2.37	3.31	0.30
1010-10	187	2.7	2.68	4.26	0.23

cance to study the crystallization kinetics under nonisothermal conditions, particularly for a material with potential value for application. Figure 4 shows the crystallization exothermic peaks (T_p's) of neat nylon 10,10 and the nylon 10,10–MMT nanocomposites at a cooling rate of 10°C/min. The integration of the exothermic peak during the nonisothermal scan gave relative crystallinity as a function of temperature (shown in Fig. 5). A series of reversed *S*-shaped curves

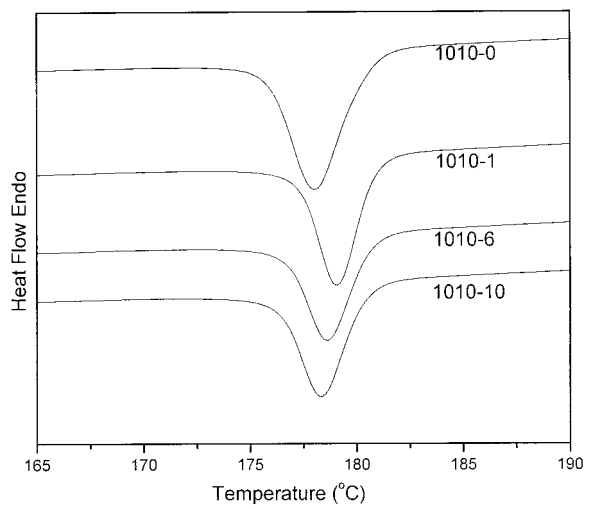

Figure 4 Heat flow versus temperature during the nonisothermal crystallization of 1010-0, 1010-1, 1010-6, and 1010-10 at a cooling rate of 10°C/min by DSC.

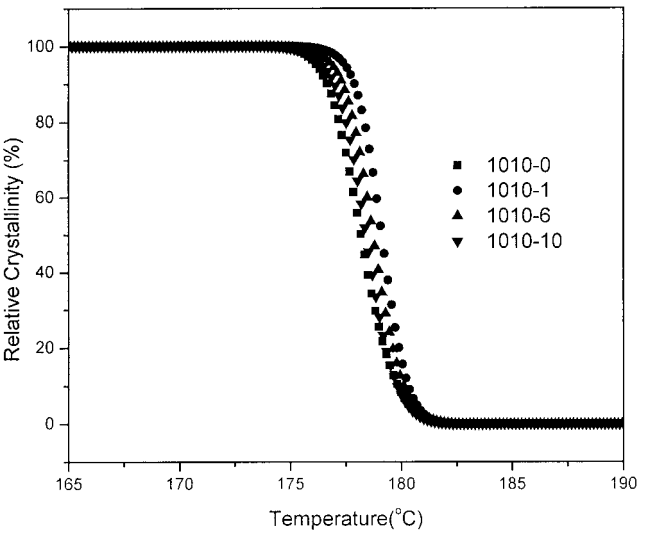

Figure 5 *Xt* at different T_c's in the process of nonisothermal crystallization for 1010-0, 1010-1, 1010-6, and 1010-10.

were obtained. The values of T_p and the crystallization enthalpies (ΔH_c's) are listed in Table II. The addition of MMT accelerated the crystallization of nylon 10,10, which indicates that the MMT particles acted as a heterophase nucleating agent. This was confirmed by the increase in crystallization temperature, T_p. Concurrently, when the MMT content was high (6 and 10 wt %), the values of T_p decreased compared with the nanocomposite with a lower MMT content (1010-1), so the effect of physical hindrance became obvious, which decreased the rate of crystallization and T_c compared with those of 1010-1. These results are in accord with the previous data. However, ΔH_c of nylon 10,10 almost remained constant, which implies that the addition of MMT did not change the extent of crystallization of nylon 10,10.

Crystal morphology analysis

The crystal morphologies of neat nylon 10,10 and nylon 10,10–MMT nanocomposites are shown in Figure 6. The neat nylon 10,10, which isothermally crystallized at 182°C [Fig. 6(A)], displayed larger and fewer spherulites compared with the nanocomposite isothermally crystallized at the same temperature [Fig. 6(B)].

TABLE II
Parameters for Nonisothermal Crystallization

	Sample			
	1010-0	1010-1	1010-6	1010-10
T_p (°C)	178.0	179.1	178.6	178.4
ΔH_c (J/g)[a]	41.08	39.14	38.65	39.52

[a] Calculated by $\Delta H_c/(1 -$ MMT content wt %) due to the presence of MMT.

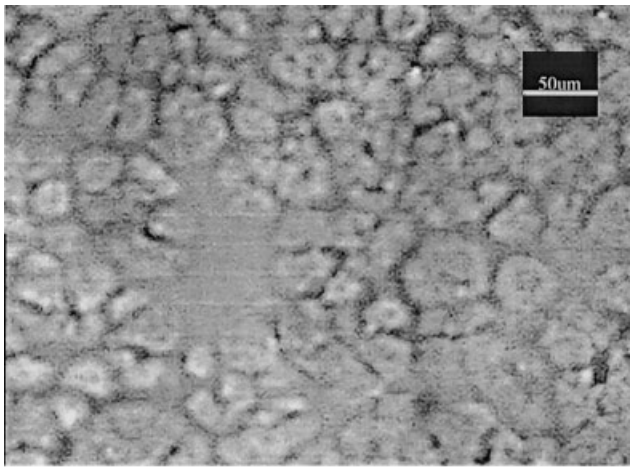

(A)

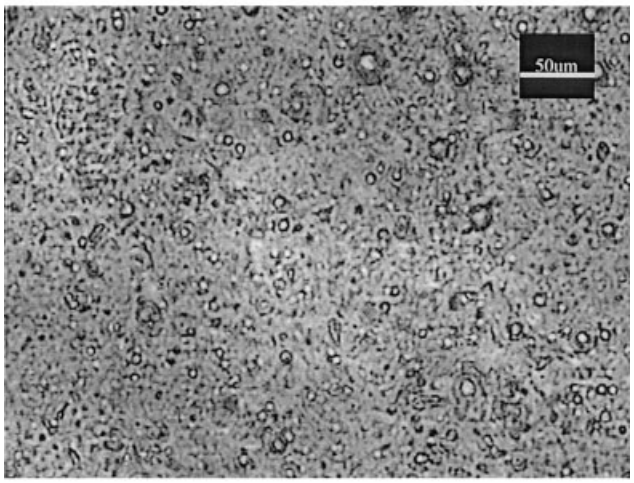

(B)

Figure 6 Polarized optical micrographs for (A) neat nylon 10,10 and (B) a nylon 10,10–MMT nanocomposite heated to 230°C for 10 min and then cooled to 182°C, at which time the samples were isothermally crystallized for 30 min.

From a comparison of the two, one can see that the MMT particles in the nanocomposite played a strong nucleation and physical hindrance role, which increased the quantity of spherulites and decreased the size of them.

Melting behavior analysis

Figure 7 shows a set of DSC heating thermograms for nylon 10,10 and the nylon 10,10–MMT nanocomposites that were collected at a heating rate of 10°C/min after nonisothermal crystallization to 50°C at 10°C/min. All the DSC curves showed double melting peaks, which reflects the so-called multiple melting behavior coined for nylons[15–24] previously. Moreover, the temperature of the low melting peak (peak I) was independent of the MMT content and stayed almost constant, whereas the temperature of high melting peak (peak II) decreased with increasing MMT content.

The heating DSC curves of nylon 10,10 and the nanocomposites isothermally crystallized at specified temperatures for 30 min at a rate of 10°C/min are shown in Figure 8. All the DSC curves also exhibited double melting peaks at the high temperature side, which was similar to the result obtained under nonisothermal crystallization conditions. Also, the low melting peak (peak I) shifted to a higher temperature as the crystallization temperature increased, and meanwhile, the high melting peak (peak II) remained almost constant.

The double melting behavior of nylon 10,10 could be attributed to recrystallization phenomena during heating;[25,28] that is, peak I was due to the melting of the material crystallized previously, and peak II corresponded to the melting of the recrystallization materials. With the increase of the isothermal crystallization temperature, the crystals became thickened and more perfect, so the temperature of peak I was enhanced. On heating, the less stable crystals melted to a supercooled state where recrystallization could occur very rapidly with the formation of better crystals. The final melting of the recrystallized material took place at the same temperature, regardless of the isothermal crystallization temperature. An endothermic peak close to the isothermal crystallization temperature (at about T_c + 3°C) is also shown in Figure 8; this was believed to be due to the annealing effects in the crystallization process. It resulted from the melting of crystals that were noncrystallized materials between bundles of lamellae initially and finally formed as thin and very defective crystal aggregates.

Figure 9 shows the temperatures of peak I and peak II as a function of MMT content. The temperature of

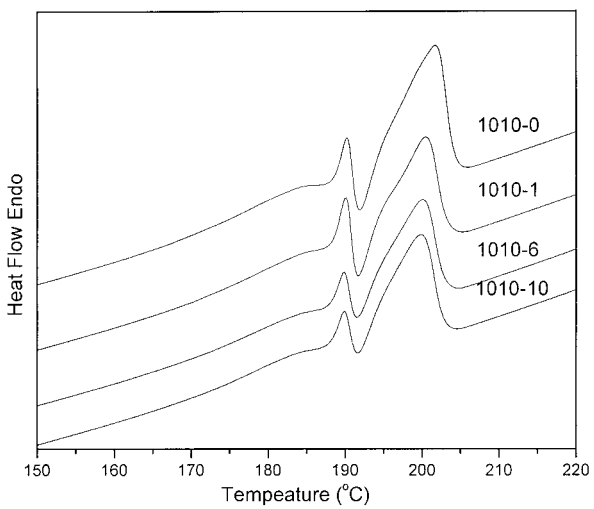

Figure 7 DSC heating thermograms for 1010-0, 1010-1, 1010-6, and 1010-10 at a heating rate of 10°C/min.

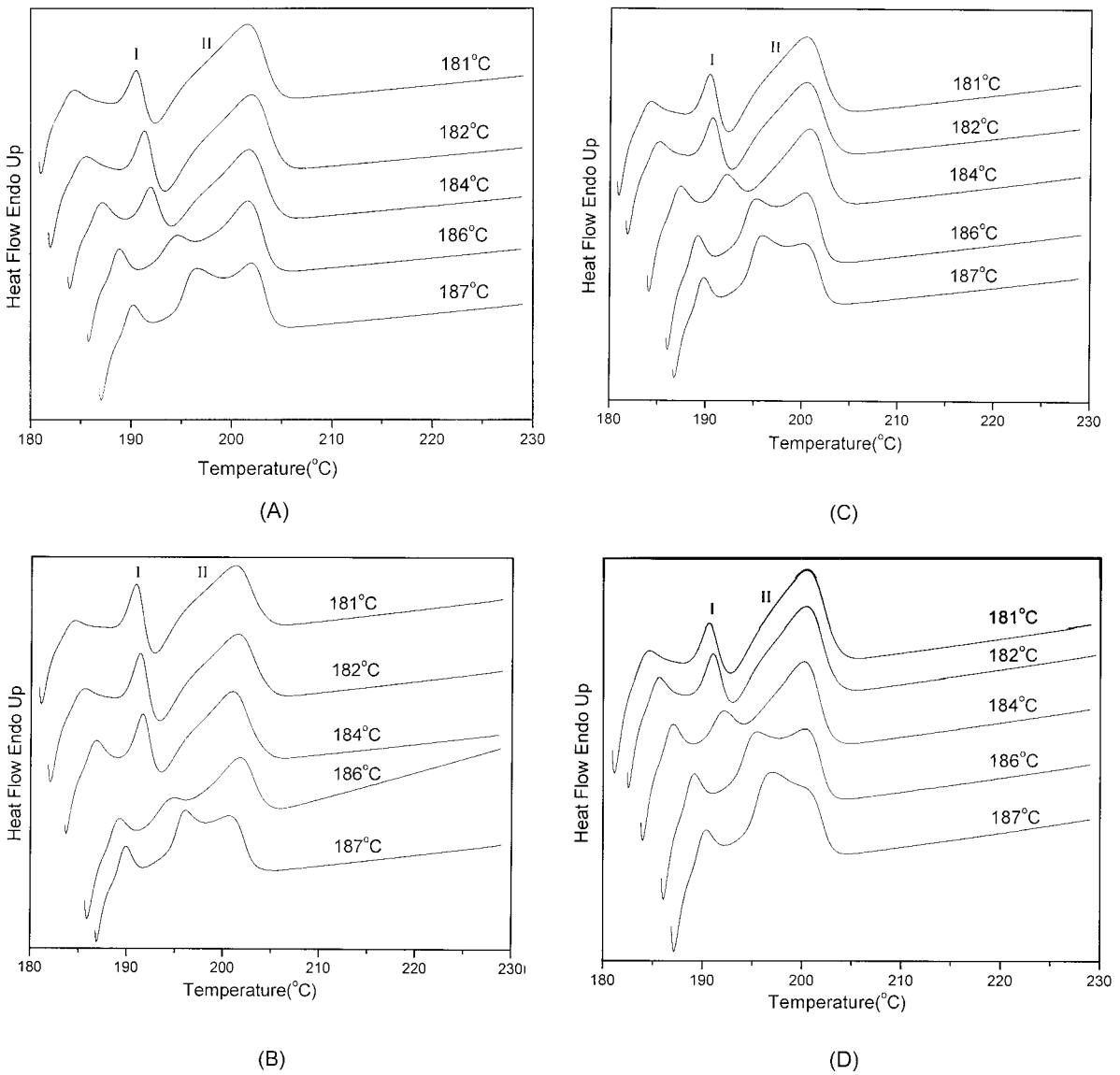

Figure 8 DSC curves of (A) 1010-0, (B) 1010-1, (C) 1010-6, and (D) 1010-10 isothermally crystallized at the indicated temperatures for 30 min. The heating rate was 10°C/min.

peak I did not depend on the MMT content; on the contrary, the temperature of peak II decreased with increasing MMT content. The crystallization kinetics data show that the presence of MMT silicate layers confined the motion of nylon 10,10 chains. Concurrently, the peak of high temperature (peak II) corresponded to the melting of the thickened, more perfect, and stable recrystallized materials. Apparently, the physical hindrance of MMT affected peak II more than peak I. So it is conceivable that peak II increased, and peak I remained constant. With increasing MMT content, nylon 10,10 chains were more restricted and difficult to recrystallize into thickened, perfect, and stable crystals, so the melting point of recrystallized material decreased, and peak II shifted to lower temperatures. However, the effect the physical hindrance played on peak I was less compared with peak II, so the temperature of peak I was independent of the MMT content and almost remained constant, and the temperature of peak II decreased with increasing MMT content. It is worth noting that the temperature of peak II did not decrease linearly with increasing MMT content, which may have originated from the random but not uniform dispersion of MMT layers.

CONCLUSIONS

The Avrami equation could be used to describe the isothermal crystallization of nylon 10,10 in neat nylon 10,10 and nylon 10,10–MMT nanocomposites. The data obtained from the analysis of isothermal process show that the addition of MMT facilitated the crystal-

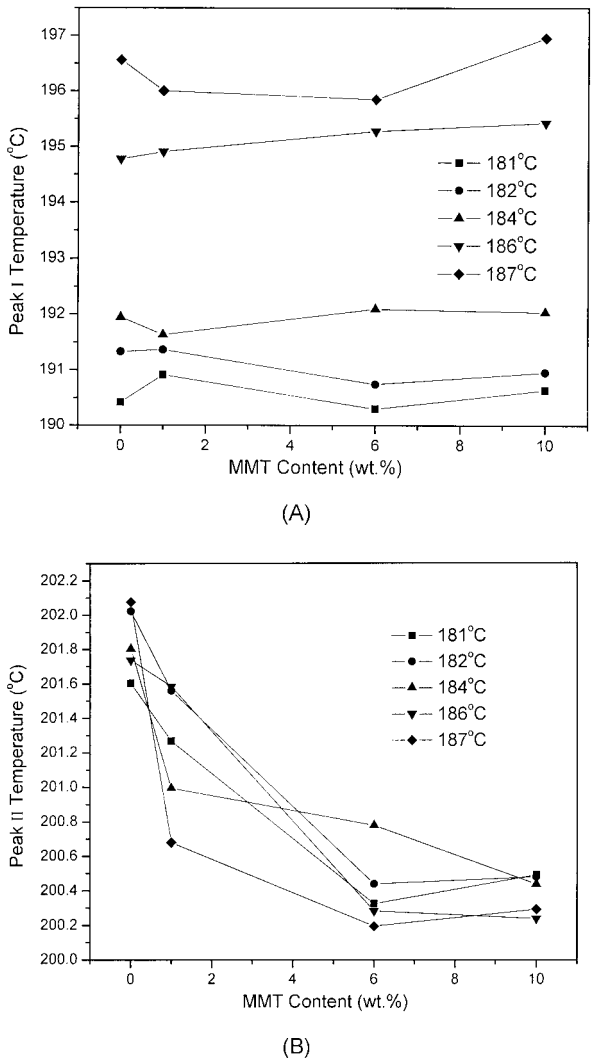

Figure 9 Temperature of (A) peak I and (B) peak II for 1010-0, 1010-1, 1010-6, and 1010-10 taken as a function of MMT content.

lization of nylon 10,10 because MMT could be considered a heterophase nucleating agent. However, when the content of MMT was high, the physical hindrance of MMT layers to the motion of nylon 10,10 chains retarded the crystallization of nylon 10,10. Polarized optical microscopy also confirmed this result.

Both nylon 10,10 and nylon 10,10–MMT nanocomposites exhibited multiple melting behavior under isothermal and nonisothermal crystallization conditions. The temperature of the lower melting peak (peak I), resulting from the melting of lamellae with different thicknesses under different conditions, was independent of the MMT content and almost remained constant, whereas the highest melting temperature (peak II), originating from the melting of the recrystallized crystals, decreased with increasing MMT content due to the physical hindrance of MMT layers to the motion of nylon 10,10 chains.

This work was sponsored by the Special Funds for Major State Basic Research Projects (G1999064802).

References

1. Usuki, A.; Kojima, Y.; Kawasumi, M.; Okada, A.; Fukushima, Y.; Kurauchi, T.; Kamigaito, O. J Mater Res 1993, 8, 1179.
2. Kojima, Y.; Usuki, A.; Kawasumi, M.; Okada, A.; Fukushima, Y.; Kurauchi, T.; Kamigaito, O. J Mater Res 1993, 8, 1185.
3. Li, L.; Qi, Z.; Zhu, X. J Appl Polym Sci 1999, 71, 1133.
4. Cho, J. W.; Paul, D. R. Polymer 2001, 42, 1083.
5. Reichert, P.; Kressler, J.; Thomann, R.; Mülhaupt, R.; Stöppelmann, G. Acta Polym 1998, 49, 116.
6. Kojima, Y.; Usuki, A.; Kawasumi, M.; Okada, A.; Kurauchi, T.; Kamigaito, O. J Appl Polym Sci 1993, 49, 1259.
7. Gilman, J. W. Appl Clay Sci 1999, 15, 31.
8. Mo, Z.; Meng, Q.; Feng, J.; Zhang, H.; Chen, D. Polym Int 1993, 32, 53.
9. Zhang, G.; Li, Y.; Yan, D.; Xu, Y. Polym Eng Sci, to appear.
10. Liu, S.; Yu, Y.; Zhang, H.; Mo, Z. J Appl Polym Sci 1998, 70, 2371.
11. Wang, G.; Yan, D. Chin J Polym Sci 1998, 16, 241.
12. Liu, J.; Mo, Z. Chin Polym Bull 1991, 4, 199.
13. Ziabicki, A. Appl Polym Symp 1967, 6, 1.
14. Li, Y.; Zhu, X.; Yan, D. Polym Eng Sci 2000, 40, 1989.
15. Won, J. C.; Fulchiron, R.; Douillard, A.; Chabert, B.; Varlet, J.; Chomier, D. Polym Eng Sci 2000, 40, 2058.
16. White, T. R. Nature 1953, 175, 895.
17. Ke, B.; Sisko, A. W. J Polym Sci 1961, 50, 87.
18. Hybart, F. J.; Plat, J. D. J Appl Polym Sci 1967, 11, 1449.
19. Bell, J. P.; Slade, P. E.; Dumbleton, J. H. J Polym Sci Part A-2: Polym Phys 1968, 6, 1773.
20. Illers, K. H.; Haberkorn, H. Makromol Chem 1971, 142, 31.
21. Ceccorulli, G.; Momescalchi, F.; Pizzoli, M. Makromol Chem 1975, 176, 1163.
22. Ishikawa, T.; Nagai, S. J Polym Sci Polym Phys Ed 1980, 18, 1413.
23. Ramesh, C.; Keller, A.; Eltink, S. J. E. A. Polymer 1994, 35, 5300.
24. Franco, L.; Puiggali, J. J Polym Sci Part B: Polym Phys 1995, 33, 2065.
25. Li, Y.; Zhu, X.; Tian, G.; Yan, D.; Zhou, E. Polym Int 2001, 50, 677.
26. Avrami, M. J Chem Phys 1939, 7, 1103.
27. Avrami, M. J Chem Phys 1940, 8, 212.
28. Lee, Y.; Porter, R. S.; Lin, J. S. Macromolecules 1989, 22, 1754.